Eur. Phys. J. C (2019) 79:863
https://doi.org/10.1140/epjc/s10052-019-7373-4

THE EUROPEAN PHYSICAL JOURNAL C

Regular Article - Theoretical Physics

Probing new physics in semileptonic $\Xi_b \to \Lambda(\Xi_c)\tau^-\bar{\nu}_\tau$ decays

Jiao Zhang[a], **Xiuyun An, Ruirui Sun, Jianfeng Su**

Department of Mathematics and Physics, Luoyang Institute of Science and Technology, Luoyang 471023, China

Received: 13 June 2019 / Accepted: 6 October 2019 / Published online: 21 October 2019

Abstract Recently, several observed anomalies in semileptonic B meson decays have implied hints of lepton flavor universal violation. Motivated by these inspiring results, we study the baryon decays $\Xi_b \to \Lambda(\Xi_c)\tau^-\bar{\nu}_\tau$ which are mediated by $b \to u(c)\tau^-\bar{\nu}_\tau$ transitions at quark level in the Standard Model and different New Physics scenarios. In the framework of the extended Standard Model on assuming a general effective theory, we constrain the Wilson coefficients of the NP operators using the experimental measurement results for the $Br(B_c^+ \to \tau^+\nu_\tau)$, R_π^l, $R_{D^{(*)}}$, $R_{J/\psi}$ and $F_L^{D^*}$ anomalies and investigate their New Physics effects on several observables relative to the $\Xi_b \to \Lambda(\Xi_c)\tau^-\bar{\nu}_\tau$ decays. We mention the differential branching fraction $\mathrm{d}Br/\mathrm{d}q^2$, the ratio of branching fractions $R(q^2)$, the lepton-side forward–backward asymmetry $A_{FB}(q^2)$, the longitudinal polarization $P_L^{\Lambda(\Xi_c)}(q^2)$ of the daughter baryons $\Lambda(\Xi_c)$ and $P_L^\tau(q^2)$ of the τ lepton, and the convexity parameter $C_F(q^2)$.

1 Introduction

In the Standard Model (SM), the gauge interactions are lepton flavor universal (LFU), but the hints of lepton flavor universal violation (LFUV) have been observed in several anomalies relative to the semileptonic B meson decays. The Belle [1–3], BaBar [4,5] and LHCb [6–8] collaborations have reported $R_{D^{(*)}}$ and $R_{J/\psi}$ anomalies in various semileptonic B meson decays mediated by $b \to c$ charged current interactions. The experimental measurement results for these anomalies show large deviations with their corresponding SM predictions, which may imply the LFUV and the existence of New Physics. The ratios are

$$R_{D^{(*)}} = \frac{Br(B \to D^{(*)}\tau^-\bar{\nu}_\tau)}{Br(B \to D^{(*)}l^-\bar{\nu}_l)}, \tag{1}$$

with $l = e, \mu$. Very recently, the Belle collaboration announced the latest measurements of $R_{D^{(*)}}$ [9],

$$R_D^{\mathrm{Bell}} = 0.307 \pm 0.037 \pm 0.016,$$
$$R_{D^*}^{\mathrm{Bell}} = 0.283 \pm 0.018 \pm 0.014, \tag{2}$$

which agree with their SM predictions within 1.2σ in combination. Although the tension between the new results and the SM predictions is obviously reduced, it still amounts to 3.08σ relative to the corresponding SM predictions on combining these measurements in the global average fields, and the new average values reported by the Heavy Flavor Average Group (HFAG) are [10]

$$R_D^{\mathrm{avg}} = 0.340 \pm 0.027 \pm 0.013,$$
$$R_{D^*}^{\mathrm{avg}} = 0.295 \pm 0.011 \pm 0.008, \tag{3}$$

which deviate from their SM predictions at 1.4σ and 2.5σ level, respectively. The SM predictions for $R_{D^{(*)}}$ are [10]

$$R_D^{\mathrm{SM}} = 0.299 \pm 0.003, \quad R_{D^*}^{\mathrm{SM}} = 0.258 \pm 0.005. \tag{4}$$

Another anomaly,

$$R_{J/\psi} = \frac{Br(B^+ \to J/\psi\tau^+\nu_\tau)}{Br(B^+ \to J/\psi\mu^+\mu_\tau)} = 0.71 \pm 0.17 \pm 0.18, \tag{5}$$

was reported by [8] and deviated from the central value predicted in the SM 0.25–0.28 within 2σ range [11,12].

In addition, there is also discrepancy in the measured ratio [13]

$$R_\pi^l = \frac{\tau_{B^0}}{\tau_{B^-}} \frac{Br(B^- \to \tau^-\bar{\nu}_\tau)}{Br(B^0 \to \pi^+l^-\bar{\nu}_l)} = 0.699 \pm 0.156, \tag{6}$$

with $l = e, \mu$, which also attracts our attention. The experimental result has about 1σ tension with its SM prediction, 0.583 ± 0.055.

Except for the tensions mentioned above, we also investigate the effects of the very recently announced value for

[a] e-mail: zhangjiao198746@163.com

D^* longitudinal polarization $F_L^{D^*}$ by the Belle collaboration [14],

$$F_L^{D^*} = \frac{\Gamma_{\lambda_{D^*}=0}(B \to D^* \tau^+ \nu_\tau)}{\Gamma(B \to D^* \tau^+ \nu_\tau)} = 0.60 \pm 0.08 \pm 0.04, \quad (7)$$

which differs from its SM prediction, 0.457 ± 0.010 [15] (0.441 ± 0.006 [16]), by $1.6\sigma (1.8\sigma)$.

It is really interesting and important to investigate the semileptonic baryon decays $\Xi_b \to \Lambda(\Xi_c)\tau^-\bar{\nu}_\tau$ mediated by the $b \to u(c)\tau^-\bar{\nu}_\tau$ transitions at the quark level. Studying them not only can provide an independent determination of the Cabibbo–Kobayashi–Maskawa (CKM) matrix elements $|V_{ub}|$ and $|V_{cb}|$, but also it may confirm the LFUV again in the ratios of branching fractions $R_{\Lambda(\Xi_c)}$ having a similar formalism to the $R_{D^{(*)}}$. On the basis of these advantages, many researchers have studied the decays $\Xi_b \to \Lambda(\Xi_c)\tau^-\bar{\nu}_\tau$ in the SM and NP scenarios [17–24]. In this paper, we set out to explore the NP effects of these B meson decay anomalies in the $\Xi_b \to \Lambda(\Xi_c)\tau^-\bar{\nu}_\tau$ transitions. Using the Wilson coefficients of the NP operators constrained from the experimental values for $Br(B_c^+ \to \tau^+\nu_\tau)$, the R_π^l, $R_{D^{(*)}}$, $R_{J/\psi}$ and $F_L^{D^*}$ anomalies and the form factors for the $\Xi_b \to \Lambda(\Xi_c)$ transitions calculated by [24], we investigate the NP effects of these anomalies on the differential branching fraction $\mathrm{d}Br/\mathrm{d}q^2$, the ratio of branching fractions $R(q^2)$, the lepton-side forward–backward asymmetry $A_{FB}(q^2)$, the longitudinal polarization $P_L^{\Lambda(\Xi_c)}(q^2)$ of the daughter baryons $\Lambda(\Xi_c)$ and $P_L^\tau(q^2)$ of the τ lepton, and the convexity parameter $C_F^l(q^2)$ relative to these baryon decays. It is worthwhile to note that our study is different from [23] whose authors also investigate the decay $\Xi_b \to \Xi_c\tau^-\bar{\nu}_\tau$ using a model-independent approach. We make the Wilson coefficients complex, though they are real in [23], and also we consider the constraints on the NP Wilson coefficients coming from $R_{J/\psi}$ and $F_L^{D^*}$ anomalies, which are not mentioned in [23]. In [13], the authors also consider the constraints on the complex NP Wilson coefficients, but they treat the $b \to u$ and $b \to c$ transitions separately. Therefore, the constraints on the NP Wilson coefficients are different from ours as is appropriate for both the $b \to u$ and the $b \to c$ transitions. In addition, we also consider the interplay of vector and scalar interactions scenarios, which are not mentioned in [13,23]. In this paper, we consider the $b \to u$ and $b \to c$ transitions together in the same framework of effective theory and perform a combined analysis using the constraints on the Wilson coefficients coming from the experimental results for the $Br(B_c^+ \to \tau^+\nu_\tau)$, R_π^l, $R_{D^{(*)}}$, $R_{J/\psi}$ and $F_L^{D^*}$ anomalies in the end in determining the NP contributions to the observables aforementioned.

Our paper is organized as follows. In Sect. 2, we introduce the effective theory describing the $b \to u(c)l^-\bar{\nu}_\tau$ transitions as well as the form factors, the helicity amplitudes and the observables of the $\Xi_b \to \Lambda(\Xi_c)l^-\bar{\nu}_\tau$ decays. In Sect. 3, the Wilson coefficients of the NP operators are constrained from the experimental values for $Br(B_c^+ \to \tau^+\nu_\tau)$, R_π^l, $R_{D^{(*)}}$, $R_{J/\psi}$ and $F_L^{D^*}$ anomalies. In Sect. 4, the numerical results for the observables $\mathrm{d}Br/\mathrm{d}q^2$, $R(q^2)$, $A_{FB}(q^2)$, $P_L^{\Lambda(\Xi_c)}(q^2)$, $P_L^\tau(q^2)$ and $C_F^l(q^2)$ in the SM and different NP scenarios are presented. Finally, we briefly conclude in Sect. 5.

2 Effective Hamiltonian, form factors, helicity amplitude and observables for $\Xi_b \to \Lambda(\Xi_c)l^-\bar{\nu}_\tau$ decays

2.1 Effective Hamiltonian

The effective Hamiltonian including both the SM and the NP contributions for the $b \to ql^-\bar{\nu}_\tau$, $(q = u, c)$ transitions is given by [25,26],

$$\begin{aligned}\mathcal{H}_{\rm eff} = &-\frac{4G_F}{\sqrt{2}} V_{qb} \{(1 + V_L)\bar{l}_L\gamma_\mu\nu_L\bar{q}_L\gamma^\mu b_L \\ &+V_R\bar{l}_L\gamma_\mu\nu_L\bar{q}_R\gamma^\mu b_R + S_L\bar{l}_R\nu_L\bar{q}_R b_L \\ &+S_R\bar{l}_R\nu_L\bar{q}_L b_R + T_L\bar{l}_R\sigma_{\mu\nu}\nu_L\bar{q}_R\sigma^{\mu\nu}b_L\} + h.c.,\end{aligned} \quad (8)$$

where G_F is the Fermi constant, V_{qb} are the CKM matrix elements and $(q, b, l, \nu)_{L,R} = \frac{1\mp\gamma_5}{2}(q, b, l, \nu)$. The vector, scalar and tensor type NP couplings are denoted $V_{L,R}$, $S_{L,R}$ and T_L, respectively. They are all zero in the SM, and we have assumed that there are only left-handed neutrinos. The right-handed quark current for the tensor operator is omitted because of its zero value. In addition, the NP effects are supposed to appear only in the τ mode in Eq. (8). This paper we dedicate to a study of the vector and scalar type interactions, excepting the tensor interaction, and we assume that the Wilson coefficients $V_{L,R}$ and $S_{L,R}$ are complex.

2.2 Form factors

The hadronic matrix elements of the vector and axial-vector weak currents for the decays $\Xi_b \to \Lambda(\Xi_c)l^-\bar{\nu}_\tau$ are parametrized in terms of the six invariant form factors $f_{1,2,3}$ and $g_{1,2,3}$ [24,27–29],

$$\begin{aligned}&\langle\Lambda(\Xi_c), \lambda_2|\bar{u}(\bar{c})\gamma_\mu b|\Xi_b, \lambda_1\rangle = \bar{u}_{\Lambda(\Xi_c)}(p_2, \lambda_2) \\ &\times \left[f_1(q^2)\gamma_\mu - if_2(q^2)\sigma_{\mu\nu}\frac{q^\nu}{M_{\Xi_b}} + f_3(q^2)\frac{q_\mu}{M_{\Xi_b}}\right] \\ &u_{\Xi_b}(p_1, \lambda_1), \\ &\times\langle\Lambda(\Xi_c), \lambda_2|\bar{u}(\bar{c})\gamma_\mu\gamma_5 b|\Xi_b, \lambda_1\rangle = \bar{u}_{\Lambda(\Xi_c)}(p_2, \lambda_2) \\ &\times \left[g_1(q^2)\gamma_\mu - ig_2(q^2)\sigma_{\mu\nu}\frac{q^\nu}{M_{\Xi_b}} + g_3(q^2)\frac{q_\mu}{M_{\Xi_b}}\right] \\ &\times \gamma_5 u_{\Xi_b}(p_1, \lambda_1),\end{aligned} \quad (9)$$

where $\sigma_{\mu\nu} = \frac{i}{2}(\gamma_\mu\gamma_\nu - \gamma_\nu\gamma_\mu)$, $q = p_1 - p_2$ is the four-momentum transfer and the $\lambda_i = \pm\frac{1}{2}(i = 1, 2)$ denote the helicities of the parent baryon Ξ_b and daughter baryons $\Lambda(\Xi_c)$, respectively. Using the equations of motion, we can obtain the hadronic matrix elements of the scalar and pseudo-scalar currents between the two baryons. The expressions for them are

$$\begin{aligned}\langle\Lambda(\Xi_c),\lambda_2|\bar{u}(\bar{c})b|\Xi_b,\lambda_1\rangle &= \frac{1}{m_b - m_{u(c)}}\bar{u}_{\Lambda(\Xi_c)}(p_2,\lambda_2)\\ &\times\left[f_1(q^2)(M_{\Xi_b} - M_{\Lambda(\Xi_c)}) + f_3(q^2)\frac{q^2}{M_{\Xi_b}}\right]u_{\Xi_b}(p_1,\lambda_1),\\ \langle\Lambda(\Xi_c),\lambda_2|\bar{u}(\bar{c})\gamma_5 b|\Xi_b,\lambda_1\rangle &= \frac{1}{m_b + m_{u(c)}}\bar{u}_{\Lambda(\Xi_c)}(p_2,\lambda_2)\\ &\times\left[g_1(q^2)(M_{\Xi_b} + M_{\Lambda(\Xi_c)}) - g_3(q^2)\frac{q^2}{M_{\Xi_b}}\right]\gamma_5 u_{\Xi_b}(p_1,\lambda_1).\end{aligned} \tag{10}$$

The form factors can be approximated with high accuracy by the following analytic expression [24]:

$$f(q^2) = g(q^2) = \frac{1}{1 - q^2/M_{\text{pole}}^2}\times\{a_0 + a_1 z(q^2) + a_2[z(q^2)]^2\}, \tag{11}$$

where we have the variable

$$z(q^2) = \frac{\sqrt{t_+ - q^2} - \sqrt{t_+ - t_0}}{\sqrt{t_+ - q^2} + \sqrt{t_+ - t_0}}, \tag{12}$$

with $t_+ = (M_{\Xi_b} + M_{\Lambda(\Xi_c)})^2$ and $t_0 = (M_{\Xi_b} - M_{\Lambda(\Xi_c)})^2$. The values of $a_{0,1,2}$ and the pole masses are given in Table 1.

2.3 Helicity amplitude and observables

The hadronic helicity amplitudes in the form of the form factors and the NP couplings are [27–29]

$$\begin{aligned}H^V_{\frac{1}{2}0} &= (1 + V_L + V_R)\frac{\sqrt{Q_-}}{\sqrt{q^2}}\\ &\times\left[(M_{\Xi_b} + M_{\Lambda(\Xi_c)})f_1(q^2) + \frac{q^2}{M_{\Xi_b}}f_2(q^2)\right],\\ H^A_{\frac{1}{2}0} &= (1 + V_L - V_R)\frac{\sqrt{Q_+}}{\sqrt{q^2}}\\ &\times\left[(M_{\Xi_b} - M_{\Lambda(\Xi_c)})g_1(q^2) - \frac{q^2}{M_{\Xi_b}}g_2(q^2)\right],\\ H^V_{\frac{1}{2}1} &= (1 + V_L + V_R)\sqrt{2Q_-}\\ &\times\left[f_1(q^2) + \frac{(M_{\Xi_b} + M_{\Lambda(\Xi_c)})}{M_{\Xi_b}}f_2(q^2)\right],\\ H^A_{\frac{1}{2}1} &= (1 + V_L - V_R)\sqrt{2Q_+}\\ &\times\left[g_1(q^2) - \frac{(M_{\Xi_b} - M_{\Lambda(\Xi_c)})}{M_{\Xi_b}}g_2(q^2)\right],\\ H^V_{\frac{1}{2}t} &= (1 + V_L + V_R)\frac{\sqrt{Q_+}}{\sqrt{q^2}}\\ &\times\left[(M_{\Xi_b} - M_{\Lambda(\Xi_c)})f_1(q^2) + \frac{q^2}{M_{\Xi_b}}f_3(q^2)\right],\\ H^A_{\frac{1}{2}t} &= (1 + V_L - V_R)\frac{\sqrt{Q_-}}{\sqrt{q^2}}\\ &\times\left[(M_{\Xi_b} + M_{\Lambda(\Xi_c)})g_1(q^2) - \frac{q^2}{M_{\Xi_b}}g_3(q^2)\right],\end{aligned}$$

Table 1 Form factors for the weak $\Xi_b \to \Lambda$ and $\Xi_b \to \Xi_c$ transitions

$\Xi_b \to \Lambda$	$f_1(q^2)$	$f_2(q^2)$	$f_3(q^2)$	$g_1(q^2)$	$g_2(q^2)$	$g_3(q^2)$
$f(0)/g(0)$	0.092	0.029	−0.002	0.077	0.007	−0.041
$f(q^2_{\text{max}})/g(q^2_{\text{max}})$	0.609	0.745	0.290	0.369	−0.528	−1.36
a_0	0.139	0.170	0.098	0.122	−0.175	−0.292
a_1	0.136	−0.368	−0.323	0.016	0.865	0.554
a_2	−0.845	−0.180	0.059	−0.470	−0.947	0.630
M_{pole}	5.325	5.325	5.749	5.723	5.723	5.280
$\Xi_b \to \Xi_c$	$f_1(q^2)$	$f_2(q^2)$	$f_3(q^2)$	$g_1(q^2)$	$g_2(q^2)$	$g_3(q^2)$
$f(0)/g(0)$	0.474	0.150	0.081	0.449	−0.030	−0.285
$f(q^2_{\text{max}})/g(q^2_{\text{max}})$	0.945	0.426	0.161	0.962	−0.104	−0.752
a_0	0.684	0.308	0.121	0.729	−0.078	−0.541
a_1	−5.16	−4.18	−0.315	−7.11	0.775	6.93
a_2	28	25.9	−5.81	41.5	0.372	−44.9
M_{pole}	6.333	6.333	6.699	6.743	6.743	6.275

$$H^S_{\frac{1}{2}0} = \frac{(S_L + S_R)\sqrt{2Q_+}}{m_b - m_{u(c)}} \times \left[(M_{\Xi_b} - M_{\Lambda(\Xi_c)}) f_1(q^2) + \frac{q^2}{M_{\Xi_b}} f_3(q^2)\right],$$
$$H^P_{\frac{1}{2}0} = \frac{(S_L - S_R)\sqrt{2Q_-}}{m_b + m_{u(c)}} \times \left[(M_{\Xi_b} + M_{\Lambda(\Xi_c)}) g_1(q^2) - \frac{q^2}{M_{\Xi_b}} g_3(q^2)\right],$$
$$H_{\lambda_2,\lambda_W} = H^V_{\lambda_2,\lambda_W} - H^A_{\lambda_2,\lambda_W}, \qquad H^{SP}_{\lambda_2,0} = H^S_{\lambda_2,0} - H^P_{\lambda_2,0},$$
$$H^V_{-\lambda_2,-\lambda_W} = H^V_{\lambda_2,\lambda_W}, \qquad H^S_{-\lambda_2,0} = H^S_{\lambda_2,0},$$
$$H^A_{-\lambda_2,-\lambda_W} = -H^A_{\lambda_2,\lambda_W}, \qquad H^P_{-\lambda_2,0} = -H^P_{\lambda_2,0}, \tag{13}$$

where $Q_\pm = (M_{\Xi_b} \pm M_{\Lambda(\Xi_c)})^2 - q^2$, λ_2 and λ_W denote the helicities of the daughter baryons $\Lambda(\Xi_c)$ and the effective (axial-)vector type current, respectively.

Including the NP contributions, the differential decay distributions for the $\Xi_b \to \Lambda(\Xi_c) l^- \bar{\nu}_\tau$ decays are written as [27–29]

$$\frac{d^2\Gamma}{dq^2 d\cos\theta_l} = \frac{G_F^2 |V_{u(c)b}|^2 q^2 \sqrt{\lambda(M^2_{\Xi_b}, M^2_{\Lambda(\Xi_c)}, q^2)}}{2 \times 512\pi^3 M^3_{\Xi_b}} \left(1 - \frac{m_l^2}{q^2}\right)^2 \left[A_1 + \frac{m_l^2}{q^2} A_2 + 2A_3 + \frac{4m_l}{\sqrt{q^2}} A_4\right] \tag{14}$$

where

$$A_1 = 2\sin^2\theta_l \left(\left|H_{\frac{1}{2},0}\right|^2 + \left|H_{-\frac{1}{2},0}\right|^2\right) + (1 - \cos\theta_l)^2 \times |H_{\frac{1}{2},1}|^2 + (1 + \cos\theta_l)^2 \left|H_{-\frac{1}{2},-1}\right|^2,$$
$$A_2 = 2\cos^2\theta_l \left(|H_{\frac{1}{2},0}|^2 + |H_{-\frac{1}{2},0}|^2\right) + \sin^2\theta_l \left(\left|H_{\frac{1}{2},1}\right|^2 + \left|H_{-\frac{1}{2},-1}\right|^2\right) + 2\left(\left|H_{\frac{1}{2},t}\right|^2 + \left|H_{-\frac{1}{2},t}\right|^2\right) - 4\cos\theta_l \mathcal{R}e\left[H_{\frac{1}{2},t}\left(H_{\frac{1}{2},0}\right)^* + H_{-\frac{1}{2},t}(H_{-\frac{1}{2},0})^*\right],$$
$$A_3 = |H^{SP}_{\frac{1}{2},0}|^2 + |H^{SP}_{-\frac{1}{2},0}|^2,$$
$$A_4 = -\cos\theta_l \mathcal{R}e[H_{\frac{1}{2},0}(H^{SP}_{\frac{1}{2},0})^* + H_{-\frac{1}{2},0}(H^{SP}_{-\frac{1}{2},0})^*] + \mathcal{R}e[H_{\frac{1}{2},t}(H^{SP}_{\frac{1}{2},0})^* + H_{-\frac{1}{2},t}(H^{SP}_{-\frac{1}{2},0})^*],$$
$$\lambda(a,b,c) = a^2 + b^2 + c^2 - 2(ab + bc + ca), \tag{15}$$

with θ_l is the angle between the directions of the parent Ξ_b baryon and l^- lepton in the dilepton rest frame. One can obtain the q^2 dependent differential decay rate by integrating over $\cos\theta_l$. The expressions of the differential branching fraction dBr/dq^2, the ratios of the branching fractions $R_{\Lambda(\Xi_c)}(q^2)$, the lepton-side forward–backward asymmetry $A_{FB}(q^2)$, the longitudinal polarization $P_L^{\Lambda(\Xi_c)}(q^2)$ of the daughter baryons $\Lambda(\Xi_c)$ and $P_L^\tau(q^2)$ of the τ lepton and the convexity parameter $C_F^l(q^2)$ are written as

$$d\Gamma/dq^2 = \int_{-1}^{1} d\cos\theta_l \frac{d^2\Gamma}{dq^2 d\cos\theta_l}, \quad dBr/dq^2 = \frac{d\Gamma/dq^2}{\Gamma_{tot}}, \tag{16}$$

$$R_{\Lambda(\Xi_c)}(q^2) \equiv \frac{Br(\Xi_b \to \Lambda(\Xi_c)\tau^-\bar{\nu}_\tau)}{Br(\Xi_b \to \Lambda(\Xi_c) l^- \bar{\nu}_l)}, \tag{17}$$

$$A_{FB}(q^2) = \frac{\int_0^1 d\cos\theta_l \frac{d^2\Gamma}{dq^2 d\cos\theta_l} - \int_{-1}^0 d\cos\theta_l \frac{d^2\Gamma}{dq^2 d\cos\theta_l}}{\int_0^1 d\cos\theta_l \frac{d^2\Gamma}{dq^2 d\cos\theta_l} + \int_{-1}^0 d\cos\theta_l \frac{d^2\Gamma}{dq^2 d\cos\theta_l}}, \tag{18}$$

$$P_L^{\Lambda(\Xi_c)}(q^2) = \frac{d\Gamma^{\lambda_2=1/2}/dq^2 - d\Gamma^{\lambda_2=-1/2}/dq^2}{d\Gamma^{\lambda_2=1/2}/dq^2 + d\Gamma^{\lambda_2=-1/2}/dq^2}, \tag{19}$$

$$P_L^\tau(q^2) = \frac{d\Gamma^{\lambda_\tau=1/2}/dq^2 - d\Gamma^{\lambda_\tau=-1/2}/dq^2}{d\Gamma^{\lambda_\tau=1/2}/dq^2 + d\Gamma^{\lambda_\tau=-1/2}/dq^2}, \tag{20}$$

$$C_F(q^2) = \frac{1}{\mathcal{H}_{tot}} \frac{d^2W(\theta_l)}{d(\cos\theta_l)^2}, \qquad \mathcal{H}_{tot} = \int_{-1}^{1} W(\theta_l) d\cos\theta_l,$$
$$W(\theta_l) = \frac{3}{8}\left[A_1 + \frac{m_l^2}{q^2} A_2 + 2A_3 + \frac{4m_l}{\sqrt{q^2}} A_4\right],$$
$$\frac{d^2W(\theta_l)}{d(\cos\theta_l)^2} = \frac{3}{4}\left(1 - \frac{m_l^2}{q^2}\right) \left[|H_{\frac{1}{2},1}|^2 + |H_{-\frac{1}{2},-1}|^2 - 2\left(|H_{\frac{1}{2},0}|^2 + |H_{-\frac{1}{2},0}|^2\right)\right], \tag{21}$$

where $d\Gamma^{\lambda_2} = \pm 1/2$ and $d\Gamma^{\lambda_\tau} = \pm 1/2$ are the helicity-dependent differential decay rates, whose expressions are given in [29].

3 Constraints on the NP Wilson coefficients

In this section, we introduce the constraints on the NP Wilson coefficients coming from the experimental results for the $Br(B_c^+ \to \tau^+\nu_\tau)$, R_π^l, $R_{D^{(*)}}$, $R_{J/\psi}$ and $F_L^{D^*}$ anomalies. We assume that all the Wilson coefficients of the NP operators are complex and we consider only one new vector (scalar) coefficient or both vector and scalar coefficients existing in Eq. (8) at a time. When using the current world average of the B_c lifetime, the upper limit on $Br(B_c^+ \to \tau^+\nu_\tau)$ is [30,31]

$$Br(B_c^+ \to \tau^+\nu_\tau) \lesssim 30\%. \tag{22}$$

The branching fraction of purely leptonic $B_c^+ \to \tau^+\nu_\tau$ decay including NP contributions is written as [31]

$$Br(B_c^+ \to \tau^+\nu_\tau) = \frac{G_F^2 |V_{cb}|^2}{8\pi} \tau_{B_c} f_{B_c}^2 m_\tau^2 M_{B_c} \left(1 - \frac{m_\tau^2}{M_{B_c}^2}\right)^2 \times \left|(1 + V_L - V_R) - \frac{M_{B_c}^2}{m_\tau(m_b + m_c)}(S_L - S_R)\right|^2, \tag{23}$$

where τ_{B_c} is the lifetime and f_{B_c} is the leptonic decay constant of B_c meson.

The differential branching fractions of the decays $B \to \pi(D)l^-\bar{\nu}_l$ are expressed as [32,33]

$$\frac{\mathrm{d}Br(B \to \pi(D)l^-\bar{\nu}_l)}{\mathrm{d}q^2} = \tau_B \frac{G_F^2|V_{u(c)b}|^2}{192\pi^3 M_B^3} q^2 \sqrt{\lambda_{\pi(D)}(q^2)}\left(1-\frac{m_l^2}{q^2}\right)^2 \times \left\{|1+V_L+V_R|^2\left[\left(1+\frac{m_l^2}{2q^2}\right)H_0^2+\frac{3}{2}\frac{m_l^2}{q^2}H_t^2\right] +\frac{3}{2}|S_L+S_R|^2H_S^2+3\mathcal{R}e[(1+V_L+V_R)(S_L^*+S_R^*)] \frac{m_l^2}{\sqrt{q^2}}H_SH_t\right\},$$

in which $\lambda_{\pi(D)}(q^2) = \lambda(M_B^2, M_{\pi(D)}^2, q^2)$ and the helicity amplitudes can be written in terms of the form factors:

$$H_0 = \sqrt{\frac{\lambda_{\pi(D)}(q^2)}{q^2}}F_+(q^2), \quad H_t = \frac{M_B^2 - M_{\pi(D)}^2}{\sqrt{q^2}}F_0(q^2), \quad H_S = \frac{M_B^2-M_{\pi(D)}^2}{m_b - m_{u(c)}}F_0(q^2), \tag{24}$$

where $F_{+,0}(q^2)$ are the form factors for the $B \to \pi(D)$ weak transitions and are given in [32,34].

The differential branching fractions of the decays $B \to D^*(J/\psi)l^-\bar{\nu}_l$ are given by [32,33,35]

$$\frac{\mathrm{d}Br(B \to D^*(J/\psi)l^-\bar{\nu}_l)}{\mathrm{d}q^2} = \tau_B \frac{G_F^2|V_{cb}|^2}{192\pi^3 M_B^3} q^2 \sqrt{\lambda_{D^*(J/\psi)}(q^2)}\left(1-\frac{m_l^2}{q^2}\right)^2 \times \left\{(|1+V_L|^2+|V_R|)^2\left[\left(1+\frac{m_l^2}{2q^2}\right)(H_{V,0}^2+H_{V,+}^2 +H_{V,-}^2)+\frac{3}{2}\frac{m_l^2}{q^2}H_{V,t}^2\right] -2\mathcal{R}e[(1+V_L)V_R^*]\left[\left(1+\frac{m_l^2}{2q^2}\right) (H_{V,0}^2+2H_{V,+}H_{V,-})+\frac{3}{2}\frac{m_l^2}{q^2}H_{V,t}^2\right] +\frac{3}{2}|S_L-S_R|^2H_S^2+3\mathcal{R}e[(1+V_L-V_R)(S_L^*-S_R^*)] \frac{m_l}{\sqrt{q^2}}H_SH_{V,t}\right\},$$

where

$$H_{V,\pm} = (M_B+M_{D^*})A_1(q^2) \mp \frac{\sqrt{\lambda_{D^*}(q^2)}}{M_B+M_{D^*}}V(q^2),$$
$$H_{V,0} = \frac{M_B+M_{D^*}}{2M_{D^*}\sqrt{q^2}}\left[-(M_B^2-M_{D^*}^2-q^2)A_1(q^2) +\frac{\lambda_{D^*}(q^2)}{(M_B+M_{D^*})^2}A_2(q^2)\right],$$
$$H_{V,t} = -\sqrt{\frac{\lambda_{D^*}(q^2)}{q^2}}A_0(q^2),$$
$$H_S \simeq -\sqrt{\frac{\lambda_{D^*}(q^2)}{m_b+m_c}}A_0(q^2), \tag{25}$$

are the hadronic helicity amplitudes for the $B \to D^*l^-\bar{\nu}_l$ decays and the form factors $V(q^2)$, $A_0(q^2)$, $A_1(q^2)$ and $A_2(q^2)$ for the $B \to D^*$ transition can be found in [32].

For the $B_c \to J/\psi l^+\nu_l$ transitions, the hadronic helicity amplitudes and the form factors can easily be found in [35,36].

The $B \to D^*\tau^+\nu_\tau$ differential decay width into the longitudinally-polarized D^* meson ($\lambda_{D^*} = 0$) is given by [37]

$$\frac{\mathrm{d}\Gamma_{\lambda_{D^*}=0}}{\mathrm{d}q^2} = \frac{G_F^2|V_{cb}|^2}{192\pi^3 M_B^3} q^2 \sqrt{\lambda_{D^*}(q^2)}\left(1-\frac{m_\tau^2}{q^2}\right)^2 \times \left\{|1+V_L-V_R|^2\left[\left(1+\frac{m_\tau^2}{2q^2}\right)^2 H_{V,0}^2+\frac{3}{2}\frac{m_\tau^2}{q^2}H_{V,t}^2\right] +\frac{3}{2}|S_L-S_R|^2H_S^2 + 3\mathcal{R}e[(1+V_L-V_R)(S_L^*-S_R^*)]\frac{m_\tau}{\sqrt{q^2}}H_SH_{V,t}\right\}; \tag{26}$$

the helicity amplitudes are in Eq. (25).

Based on these functions, we calculate the predictions of the $Br(B_c^+ \to \tau^+\nu_\tau)$, R_π^l, $R_{D^{(*)}}$, $R_{J/\psi}$ and $F_L^{D^*}$ anomalies including only one new vector (scalar) coupling or both the vector and the scalar couplings at a time and compare the results with their corresponding 2σ range of the observed experimental values, are in Sect. 1. First of all, we display the constrained range of NP Wilson coefficients V_L, V_R, S_L and S_R with real and imaginary parts in Fig. 1a–d, respectively. One can easily observe the constrained range of V_L and V_R in Fig. 1a, b. We show the constrained range of S_L and S_R more vividly in Fig. 1c, d and one can more easily notice that S_L and S_R are ruled out. The constraints coming from the $F_L^{D^*}$ anomaly are not shown in Fig. 1c, d since they cannot be parameterized regularly but still have a common range

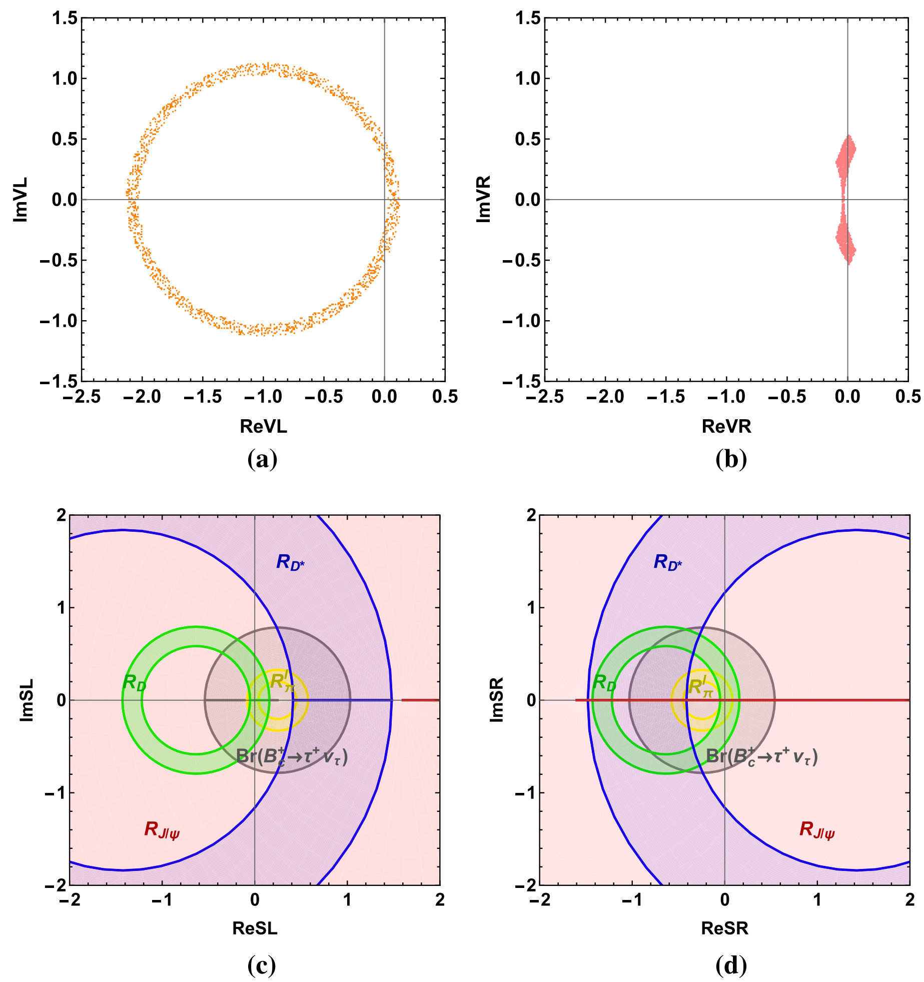

Fig. 1 The constraints on both real and imaginary parts of the NP Wilson coefficients V_L (**a**), V_R (**b**), S_L (**c**) and S_R (**d**) coming from $Br(B_c^+ \to \tau^+\nu_\tau)$, R_π^l, $R_{D^{(*)}}$, $R_{J/\psi}$ and $F_L^{D^*}$ anomalies within 2σ range of their corresponding experimental measurement results

with the other anomalies. This conclusion has been confirmed using the parameter scanning by us. The constraints on S_L coming from R_D and R_{D^*} as well as the constraints on S_R coming from R_π^l and $R_{D^{(*)}}$ have no area in common on panels c and d, respectively. Secondly, we show the constrained range of V_L and S_L, V_L and S_R, V_R and S_L, and V_R and S_R in Fig. 2a1–a4, b1–b4, c1–c4 and d1–d4, respectively. Taking the constrained range of V_L and S_L as an example, we calculate the predictions of the $Br(B_c^+ \to \tau^+\nu_\tau)$, R_π^l, $R_{D^{(*)}}$ and $F_L^{D^*}$ anomalies including the contributions of both the NP couplings V_L and S_L, and we then compare the predictions with their corresponding 2σ range of the experimental measurement values. We show the range (yellow area) of different combinations of two parameters such as ReV_L and ReS_L, ReV_L and ImS_L, ImV_L and ReS_L, and ImV_L and ImS_L, contained in the couplings V_L and S_L in Fig. 2a1–a4, respectively. From Fig. 2a1–a4, one can see that the values of ReS_L and ImS_L are in a small range compared with the values of ReV_L and ImV_L, since the NP coupling S_L is ruled out when it is considered separately.

4 Numerical results and discussions

In this section, we give the numerical results of the observables $\mathrm{d}Br/\mathrm{d}q^2$, $R(q^2)$, $A_{FB}(q^2)$, $P_L^{\Lambda(\Xi_c)}(q^2)$, $P_L^\tau(q^2)$ and $C_F^l(q^2)$ relative to the $\Xi_b \to \Lambda(\Xi_c)\tau^-\bar{\nu}_\tau$ transitions including the contributions of only NP vector type couplings and both vector and scalar type couplings except the ones of only scalar type.

Before we present the numerical results, we have to clarify the values of the SM input parameters used for the numerical calculations in Table 2.

Firstly, we suppose that the NP contributions only come from the new coefficient V_L associated with the left-handed vector like quark current. Using the constrained range within 2σ allowed for real and imaginary parts of V_L in Fig. 1a, we analyze the NP effects of V_L on the q^2 dependence of the observables $\mathrm{d}Br/\mathrm{d}q^2$, $R(q^2)$, $A_{FB}(q^2)$, $P_L^{\Lambda(\Xi_c)}(q^2)$, $P_L^\tau(q^2)$, and $C_F^l(q^2)$ and present the variations of these observables in the reasonable kinematic range in Fig. 3. The red bands represent the SM predictions and the orange bands represent the NP predictions including the contributions of

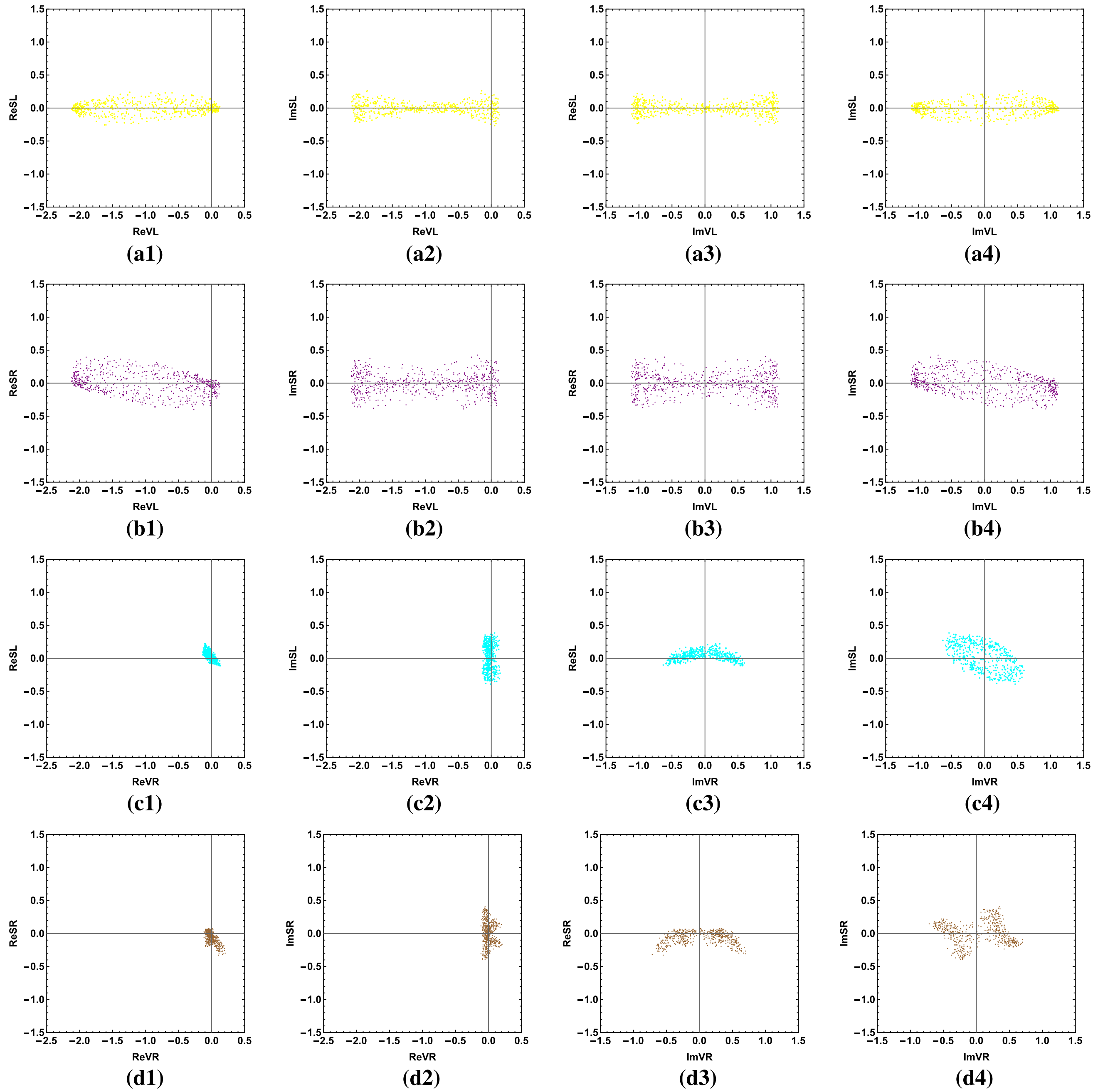

Fig. 2 The constraints on both real and imaginary parts of the NP Wilson coefficients V_L and S_L (**a1–a4**), V_L and S_R (**b1–b4**), V_R and S_L (**c1–c4**) and V_R and S_R (**d1–d4**) coming from $Br(B_c^+ \to \tau^+ \nu_\tau)$, R_π^l, $R_{D^{(*)}}$, $R_{J/\psi}$ and $F_L^{D^*}$ anomalies within 2σ range of their corresponding experimental results

V_L. The $\mathrm{d}Br/\mathrm{d}q^2$ relative to the $\Xi_b \to \Lambda(\Xi_c)\tau^- \bar{\nu}_\tau$ decays are both largely enhanced in the whole reasonable kinematic region. The red band in Fig. 3a1 is wider than that in Fig. 3b1 because of the larger uncertainty of $|V_{ub}|$ compared with $|V_{cb}|$. Additionally, the ratios $R_\Lambda(q^2)$ and $R_{\Xi_c}(q^2)$ are also largely enhanced in the whole kinematic region, especially in the large q^2 region compared with their corresponding SM predictions. Therefore, measuring the ratios $R_{\Lambda(\Xi_c)}(q^2)$ in the high kinematic region may be more useful for further

Table 2 Input parameters in the SM used for our numerical analysis [38]

$G_F = 1.166378 \times 10^{-5}$ GeV^{-2}	$m_\mu = 0.10565$ GeV
$m_\tau = 1.77682$ GeV	$m_{\Xi_b} = 5.7945$ GeV
$m_{\Xi_c} = 2.47087$ GeV	$m_\Lambda = 1.1156$ GeV
$\lvert V_{cb}\rvert = 0.0422 \pm 0.0008$	$\lvert V_{ub}\rvert = 0.00394 \pm 0.00036$

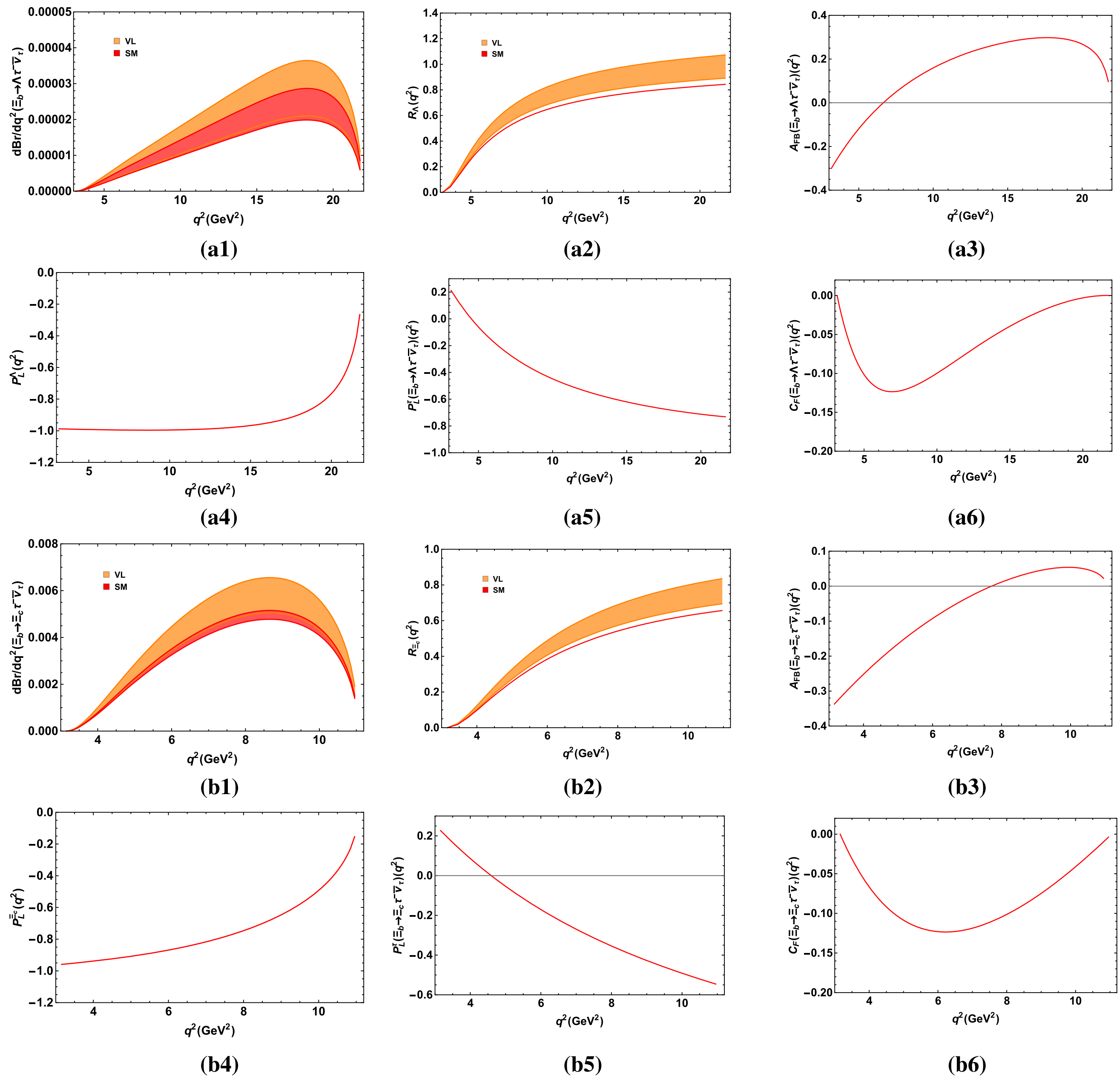

Fig. 3 The SM (red) and NP (orange) predictions in the presence of only V_L coupling for the q^2 dependent observables $\mathrm{d}Br/\mathrm{d}q^2$ (**a1**, **b1**), $R(q^2)$ (**a2**, **b2**), $A_{FB}(q^2)$ (**a3**, **b3**), $P_L^{\Lambda(\Xi_c)}(q^2)$ (**a4**, **b4**), $P_L^{\tau}(q^2)$ (**a5**, **b5**) and $C_F^l(q^2)$ (**a6**, **b6**) relative to the decays $\Xi_b \to \Lambda\tau^-\bar{\nu}_\tau$ and $\Xi_b \to \Xi_c\tau^-\bar{\nu}_\tau$, respectively. The bands contain the theoretical uncertainty of the CKM matrix elements $|V_{u(c)b}|$

confirming the NP effects of the B meson decay anomalies. We only show the SM predictions for $A_{FB}(q^2)$, $P_L^{\Lambda(\Xi_c)}(q^2)$, $P_L^{\tau}(q^2)$ and $C_F^l(q^2)$ of the two decays in Fig. 3. There is no difference between the NP predictions including contributions of V_L and the SM predictions of the $A_{FB}(q^2)$, $P_L^{\Lambda(\Xi_c)}(q^2)$, $P_L^{\tau}(q^2)$ and $C_F^l(q^2)$. Because the NP operators have the same Lorentz structure as the SM ones and the SM decay rates of the two transitions are modified by the factor $|1+V_L|^2$. The factor $|1+V_L|^2$ appears both in the numerator and in the denominator of the expressions describing $A_{FB}(q^2)$, $P_L^{\Lambda(\Xi_c)}(q^2)$, $P_L^{\tau}(q^2)$ and $C_F^l(q^2)$ simultaneously.

Secondly, using the constrained range within 2σ allowed for real and imaginary parts of the new coefficient V_R in Fig. 1b, the NP predictions including the contributions of V_R and the SM predictions for the $\mathrm{d}Br/\mathrm{d}q^2$, $R(q^2)$, $A_{FB}(q^2)$, $P_L^{\Lambda(\Xi_c)}(q^2)$, $P_L^{\tau}(q^2)$ and $C_F^l(q^2)$ relative to the $\Xi_b \to \Lambda(\Xi_c)\tau^-\bar{\nu}_\tau$ decays are displayed in Fig. 4. The

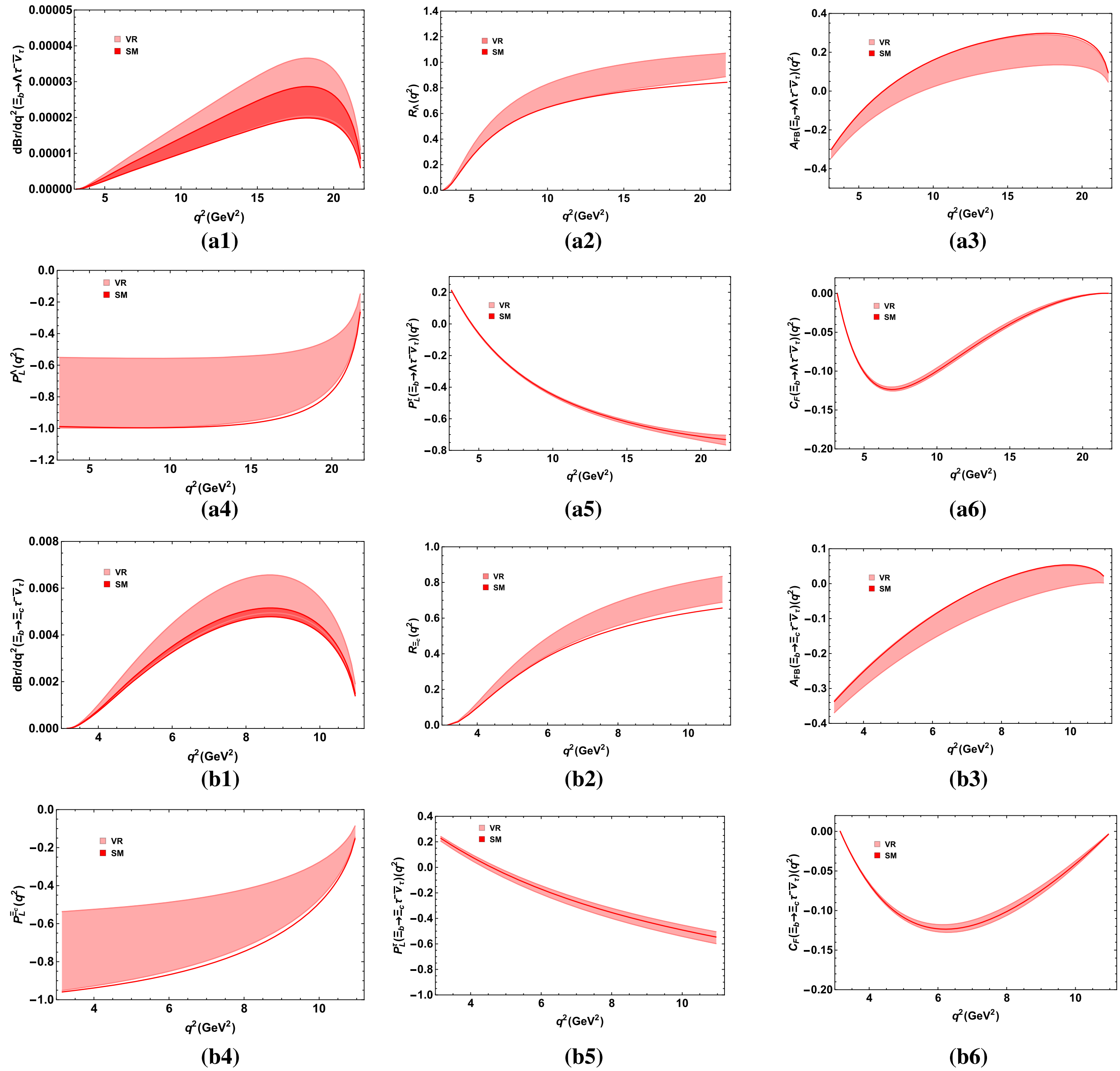

Fig. 4 The SM (red) and NP (pink) predictions in the presence of only V_R coupling for the q^2 dependent observables dBr/dq^2 (**a1**, **b1**), $R(q^2)$ (**a2**, **b2**), $A_{FB}(q^2)$ (**a3**, **b3**), $P_L^{\Lambda(\Xi_c)}(q^2)$ (**a4**, **b4**), $P_L^{\tau}(q^2)$ (**a5**, **b5**) and $C_F^{l}(q^2)$ (**a6**, **b6**) relative to the decays $\Xi_b \to \Lambda\tau^-\bar{\nu}_\tau$ and $\Xi_b \to \Xi_c\tau^-\bar{\nu}_\tau$, correspondingly. The bands contain the theoretical uncertainty of the CKM matrix elements $|V_{u(c)b}|$

red bands represent the SM predictions and the pink bands represent the NP predictions including the contributions of V_R. The NP contributions of V_R to dBr/dq^2 and $R(q^2)$ in Fig. 4a1, a2, b1, b2 have large deviations from their corresponding SM predictions in the same way as in the V_L scenario. Both dBr/dq^2 and $R(q^2)$ are enhanced in the whole reasonable kinematic region. More interesting, the NP contributions of V_R to the observables $A_{FB}(q^2)$ and $P_L^{\Lambda(\Xi_c)}(q^2)$ in Fig. 4a3, a4, b3, b4 similarly have large deviations from their SM predictions, which are really different from the scenario for V_L. The $A_{FB}(q^2)$ including NP contributions of V_R are decreased but $P_L^{\Lambda(\Xi_c)}(q^2)$ are enhanced in the whole kinematic region. The extent of the decrement and enhancement vary with the increasing of q^2. In the lowest kinematic region, the enhancement of $P_L^{\Lambda(\Xi_c)}(q^2)$ is most prominent. Therefore, it is crucial to measure $P_L^{\Lambda(\Xi_c)}(q^2)$ in the low kinematic region. Additionally, one can see that the $P_L^{\tau}(q^2)$ and $C_F^{l}(q^2)$ of these two decays including NP contributions of

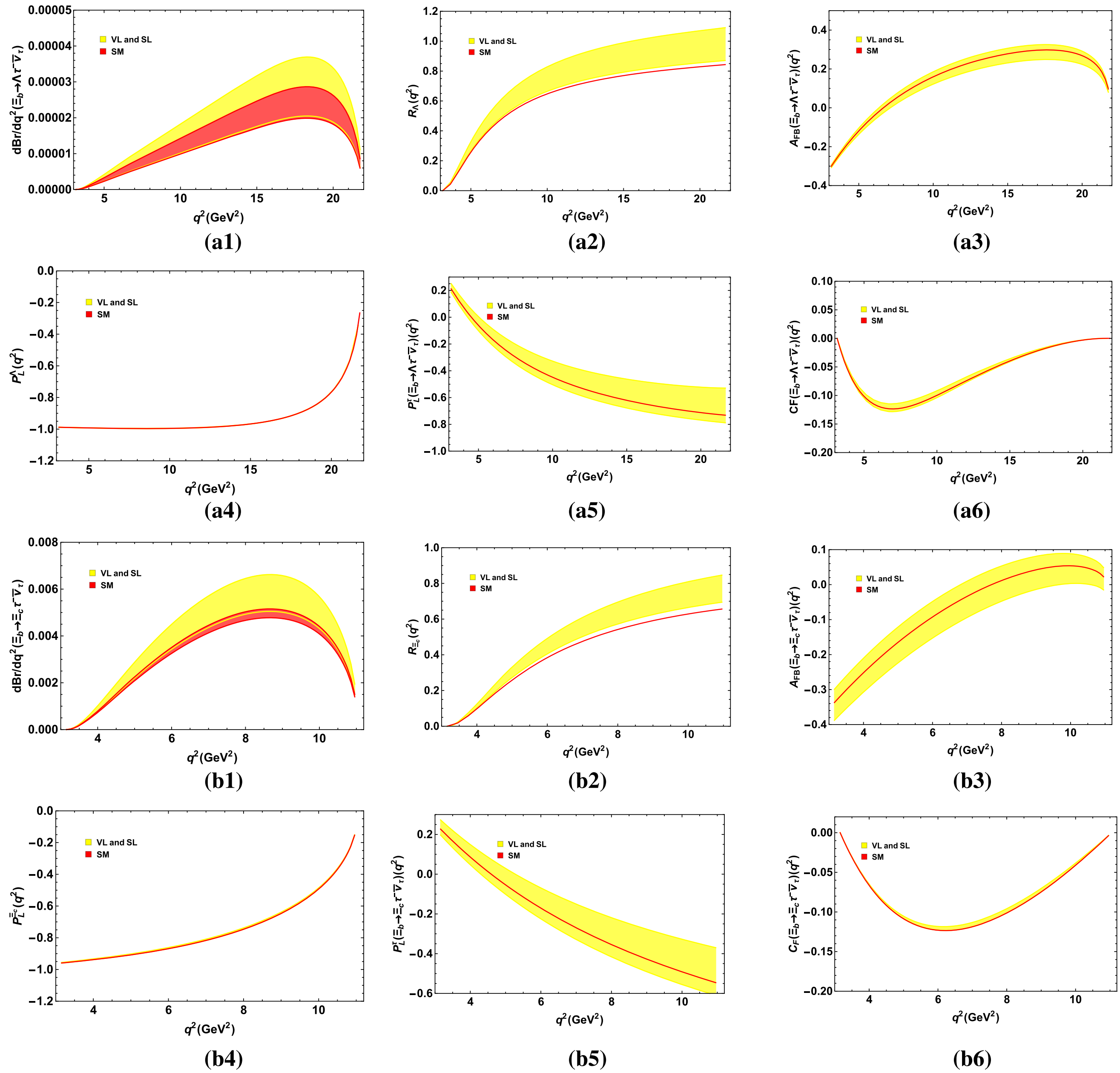

Fig. 5 The SM (red) and NP (yellow) predictions in the presence of both the V_L and the S_L couplings for the q^2 dependent observables d$Br/$dq^2 (**a1**, **b1**), $R(q^2)$ (**a2**, **b2**), $A_{FB}(q^2)$ (**a3**, **b3**), $P_L^{\Lambda(\Xi_c)}(q^2)$ (**a4**, **b4**), $P_L^\tau(q^2)$ (**a5**, **b5**) and $C_F^l(q^2)$ (**a6**, **b6**) relative to the $\Xi_b \to \Lambda\tau^-\bar{\nu}_\tau$ and $\Xi_b \to \Xi_c\tau^-\bar{\nu}_\tau$ decays, respectively. The bands contain the theoretical uncertainty of the CKM matrix elements $|V_{u(c)b}|$

V_R and their SM predictions in Fig. 4a5, a6, b5, b6 are almost the same, which indicates that they are both insensitive to the NP effects of the coupling V_R.

Finally, we show the NP contributions of four combinations of vector and scalar type couplings such as V_L and S_L, V_L and S_R, V_R and S_L, and V_R and S_R to d$Br/$dq^2, $R(q^2)$, $A_{FB}(q^2)$, $P_L^{\Lambda(\Xi_c)}(q^2)$, $P_L^\tau(q^2)$ and $C_F^l(q^2)$ relative to the $\Xi_b \to \Lambda(\Xi_c)\tau^-\bar{\nu}_\tau$ decays in Figs. 5, 6, 7 and 8. In these four figures, it is still easily to see that the NP effects of the different combinations of vector or scalar type couplings on d$Br/$dq^2 and $R(q^2)$ relative to the $\Xi_b \to \Lambda(\Xi_c)\tau^-\bar{\nu}_\tau$ decays are all similarly significant. In Fig. 5, different from the scenario only considering the NP couplings V_L, the observables $P_L^\tau(q^2)$ relative to the two decays are also sensitive to V_L and S_L. In the highest kinematic region, the deviations between the NP predictions of $P_L^\tau(q^2)$ including the contributions of V_L and S_L and the SM predictions are largest. Therefore, the observable $P_L^\tau(q^2)$ is important to dis-

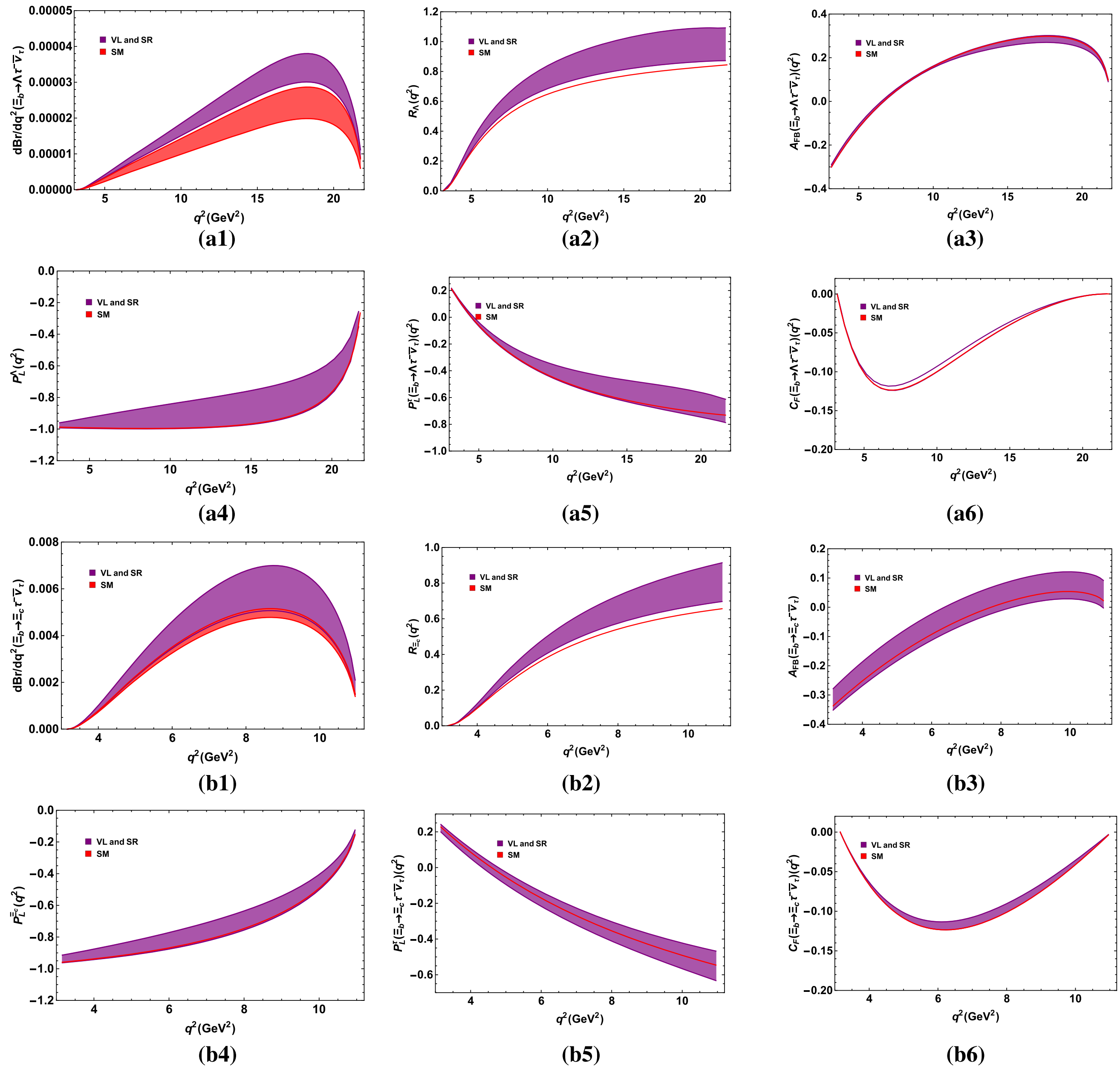

Fig. 6 The SM (red) and NP (purple) predictions in the presence of both V_L and S_R couplings for the q^2 dependent observables $\mathrm{d}Br/\mathrm{d}q^2$ (**a1**, **b1**), $R(q^2)$ (**a2**, **b2**), $A_{FB}(q^2)$ (**a3**, **b3**), $P_L^{\Lambda(\Xi_c)}(q^2)$ (**a4**, **b4**), $P_L^{\tau}(q^2)$ (**a5**, **b5**) and $C_F^l(q^2)$ (**a6**, **b6**) relative to the decays $\Xi_b \to \Lambda\tau^-\bar{\nu}_\tau$ and $\Xi_b \to \Xi_c\tau^-\bar{\nu}_\tau$, respectively. The bands contain the theoretical uncertainty of the CKM matrix elements $|V_{u(c)b}|$

tinguish the NP originating from the vector type or from both vector and scalar type couplings. In Fig. 6, except that the $\mathrm{d}Br/\mathrm{d}q^2$ and $R(q^2)$ observables are sensitive to V_L and S_R, the observables $P_L^{\Lambda(\Xi_c)}(q^2)$ are also both enhanced significantly with the NP contributions of V_L and S_R; nevertheless they are not sensitive to V_L and S_L. Once the observable $P_L^{\Lambda(\Xi_c)}(q^2)$ is measured, they can be used to distinguish the NP contributions provided by V_L and S_L or V_L and S_R. The NP predictions of the same observables in Figs. 7 and 8 show a similar variation tendency to the increasing of q^2 and have similar deviations to their corresponding SM predictions. The contributions of V_R and S_L, and V_R and S_R to the observables $\mathrm{d}Br/\mathrm{d}q^2$ and $R(q^2)$ are larger than the contributions of only V_R shown in Fig. 4. In addition, the $P_L^{\Lambda(\Xi_c)}(q^2)$ are also more sensitive to V_R and S_L, and V_R and S_R than V_R, but the contributions of V_R and S_L on $P_L^{\Lambda(\Xi_c)}(q^2)$ are a little higher than those of V_R and S_R.

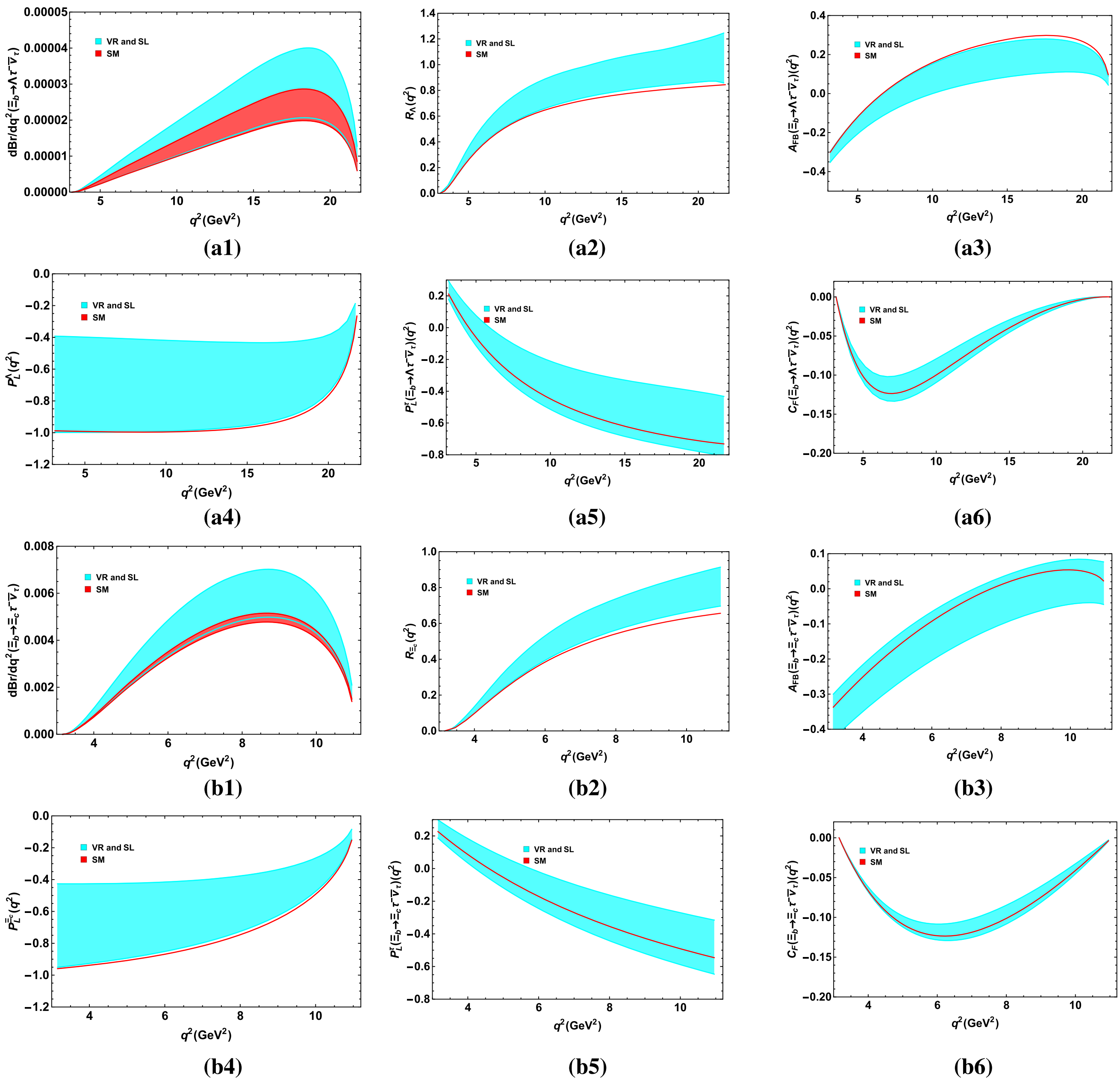

Fig. 7 The SM (red) and NP (cyan) predictions in the presence of both the V_R and the S_L couplings for the q^2 dependent observables d$Br/$dq^2 (**a1**, **b1**), $R(q^2)$ (**a2**, **b2**), $A_{FB}(q^2)$ (**a3**, **b3**), $P_L^{\Lambda(\Xi_c)}(q^2)$ (**a4**, **b4**), $P_L^{\tau}(q^2)$ (**a5**, **b5**) and $C_F^l(q^2)$ (**a6**, **b6**) relative to the decays $\Xi_b \to \Lambda\tau^-\bar{\nu}_\tau$ and $\Xi_b \to \Xi_c\tau^-\bar{\nu}_\tau$, respectively. The bands contain the theoretical uncertainty of the CKM matrix elements $|V_{u(c)b}|$

5 Summary and conclusion

Several anomalies $R_{D^{(*)}}$ and $R_{J/\psi}$ observed in the semileptonic B meson decays have indicated the hints of LFUV and attracted many researchers' attention. Much work has been done as regards the NP effects of these anomalies on the transitions mediated by the $b \to c$ charged current, such as the baryon decays $\Lambda_b \to \Lambda_c l^-\bar{\nu}_l$. It is important to investigate the semileptonic $\Xi_b \to \Lambda(\Xi_c)\tau^-\bar{\nu}_\tau$ baryon decays, which are mediated by $b \to u(c)\tau^-\bar{\nu}_\tau$ transitions at quark level. These decays not only can provide an independent determination of the CKM matrix elements $|V_{ub}|$ and $|V_{cb}|$ but also may be further confirmation of the hints of LFUV, which is helpful in exploring NP. Therefore, we investigate the $\Xi_b \to \Lambda(\Xi_c)\tau^-\bar{\nu}_\tau$ decays in the SM and various NP scenarios.

We consider the NP effects of new vector type couplings separately and the combinations of vector and scalar

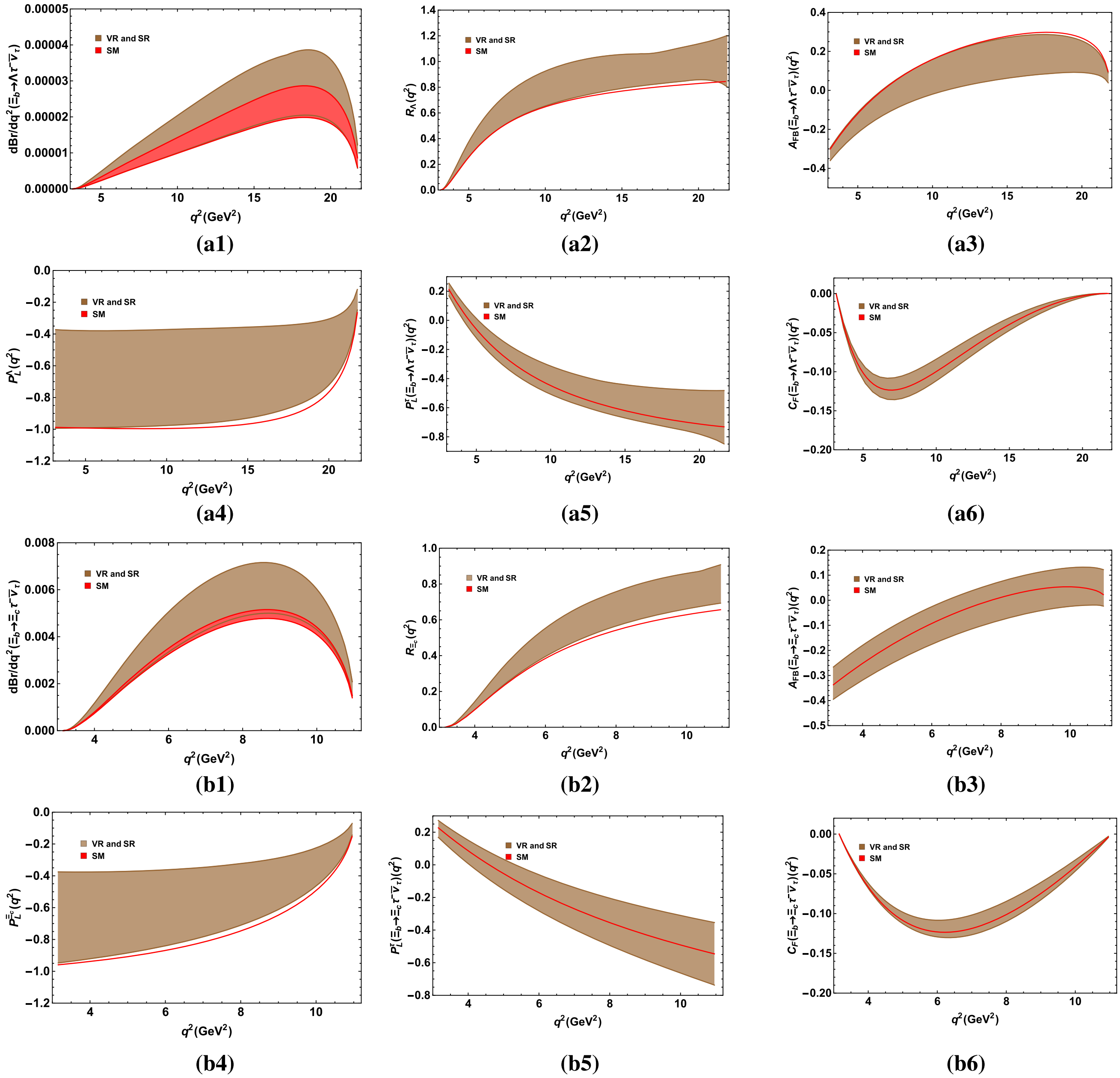

Fig. 8 The SM (red) and NP (brown) predictions in the presence of both V_R and S_R couplings for the q^2 dependent observables $\mathrm{d}Br/\mathrm{d}q^2$ (**a1**, **b1**), $R(q^2)$ (**a2**, **b2**), $A_{FB}(q^2)$ (**a3**, **b3**), $P_L^{\Lambda(\Xi_c)}(q^2)$ (**a4**, **b4**), $P_L^{\tau}(q^2)$ (**a5**, **b5**) and $C_F^l(q^2)$ (**a6**, **b6**) relative to the decays $\Xi_b \to \Lambda\tau^-\bar{\nu}_\tau$ and $\Xi_b \to \Xi_c\tau^-\bar{\nu}_\tau$, correspondingly. The bands contain the theoretical uncertainty of the CKM matrix elements $|V_{u(c)b}|$

couplings on the observables $\mathrm{d}Br/\mathrm{d}q^2$, $R(q^2)$, $A_{FB}(q^2)$, $P_L^{\Lambda(\Xi_c)}(q^2)$, $P_L^{\tau}(q^2)$ and $C_F^l(q^2)$ relative to the $\Xi_b \to \Lambda(\Xi_c)\tau^-\bar{\nu}_\tau$ transitions. The results show that $\mathrm{d}Br/\mathrm{d}q^2$ and $R(q^2)$ including any kind of NP couplings are all enhanced largely and have significant deviations comparing to their SM predictions. $A_{FB}(q^2)$, $P_L^{\Lambda(\Xi_c)}(q^2)$, $P_L^{\tau}(q^2)$ and $C_F^l(q^2)$ are the same as their corresponding SM predictions in V_L scenario, since the common coefficient $|1+V_L|^2$ appears in the numerator and the denominator of the expressions describing these observables simultaneously. Nevertheless, the contributions of V_R to the $A_{FB}(q^2)$ and $P_L^{\Lambda(\Xi_c)}(q^2)$ are also significant. In the lowest kinematic region, the enhancement of $P_L^{\Lambda(\Xi_c)}(q^2)$ is most prominent. Measuring $R(q^2)$ in the large q^2 region and $P_L^{\Lambda(\Xi_c)}(q^2)$ in the low q^2 region are more important and useful to further confirm the NP effects of the B meson decay anomalies and can be used to distinguish the new left- and right-handed vector interactions. It is worth noting that the $P_L^{\Lambda(\Xi_c)}(q^2)$ are sensitive to V_L and

S_R but not V_L and S_L, so detecting $P_L^{\Lambda(\Xi_c)}(q^2)$ is important to confirm the origin of NP effects. For the V_R and S_L and the V_R and S_R scenarios, the characters of the NP effects on $P_L^{\Lambda(\Xi_c)}(q^2)$ are similar and both are more significant than in the scenario with only V_R. In addition, the $P_L^{\tau}(q^2)$ of these two decays are both sensitive to V_R and S_L and to V_R and S_R, but not to only V_R. In this case, the observables $P_L^{\Lambda(\Xi_c)}(q^2)$ and $P_L^{\tau}(q^2)$ could be an effective target for differentiating the V_R from V_R and S_L, and from V_R and S_R. We think this investigation will be helpful in exploring and distinguishing different NP scenarios.

Acknowledgements This work was supported by the National Natural Science Foundation of China under Grants nos. 11547266 and 11905096; the Natural Science Foundation of Henan Province Grant nos. 16A140045, 16A140012 and 172102210404; the program for Youth Scholar teachers Supporting Plan in Universities of Henan province Grant no. 2018GGJS158.

Data Availability Statement This manuscript has no associated data or the data will not be deposited. [Authors' comment: The datasets during and analysed during the current study available from the corresponding author on reasonable request.]

References

1. M. Huschle et al. [Belle Collaboration], Phys. Rev. D **92**(7), 072014 (2015) arXiv:1507.03233 [hep-ex]
2. A. Abdesselam et al. [Belle Collaboration], arXiv:1603.06711 [hep-ex]
3. A. Abdesselam et al. [Belle Collaboration], arXiv:1608.06391 [hep-ex]
4. J.P. Lees et al. [BaBar Collaboration], Phys. Rev. Lett. **109**, 101802 (2012) arXiv:1205.5442 [hep-ex]
5. J.P. Lees et al. [BaBar Collaboration], Phys. Rev. D **88**(7), 072012 (2013) arXiv:1303.0571 [hep-ex]
6. R. Aaij et al. [LHCb Collaboration], Phys. Rev. Lett. **115**(11), 111803 (2015) Erratum: [Phys. Rev. Lett. **115**, no. 15, 159901 (2015)] arXiv:1506.08614 [hep-ex]
7. R. Aaij et al. [LHCb Collaboration], Phys. Rev. Lett. **120**(17), 171802 (2018) arXiv:1708.08856 [hep-ex]
8. R. Aaij et al. [LHCb Collaboration], Phys. Rev. Lett. **120**(12), 121801 (2018) arXiv:1711.05623 [hep-ex]
9. A. Abdesselam et al. [Belle Collaboration], arXiv:1904.08794 [hep-ex]
10. [Heavy Flavor Averaging Group Collaboration], https://hflav-eos.web.cern.ch/hflav-eos/semi/spring19/html/RDsDsstar/RDRDs.html
11. W.F. Wang, Y.Y. Fan, Z.J. Xiao, Chin. Phys. C **37**, 093102 (2013). arXiv:1212.5903 [hep-ph]
12. R. Dutta, A. Bhol, Phys. Rev. D **96**(7), 076001 (2017). arXiv:1701.08598 [hep-ph]
13. A. Ray, S. Sahoo, R. Mohanta, Phys. Rev. D **99**(1), 015015 (2019). arXiv:1812.08314 [hep-ph]
14. A. Abdesselam et al. [Belle Collaboration], arXiv:1903.03102 [hep-ex]
15. S. Bhattacharya, S. Nandi, S. Kumar Patra, Eur. Phys. J. C **79**(3), 268 (2019). arXiv:1805.08222 [hep-ph]
16. Z.R. Huang, Y. Li, C.D. Lu, M.A. Paracha, C. Wang, Phys. Rev. D **98**(9), 095018 (2018). arXiv:1808.03565 [hep-ph]
17. D. Ebert, R.N. Faustov, V.O. Galkin, Phys. Rev. D **73**, 094002 (2006). arXiv:hep-ph/0604017
18. R.L. Singleton, Phys. Rev. D **43**, 2939 (1991)
19. M.A. Ivanov, V.E. Lyubovitskij, J.G. Korner, P. Kroll, Phys. Rev. D **56**, 348 (1997). arXiv:hep-ph/9612463
20. M.A. Ivanov, J.G. Korner, V.E. Lyubovitskij, A.G. Rusetsky, Phys. Rev. D **59**, 074016 (1999). arXiv:hep-ph/9809254
21. C. Albertus, E. Hernandez, J. Nieves, Phys. Rev. D **71**, 014012 (2005). arXiv:nucl-th/0412006
22. J.G. Korner, M. Kramer, D. Pirjol, Prog. Part. Nucl. Phys. **33**, 787 (1994). arXiv:hep-ph/9406359
23. R. Dutta, Phys. Rev. D **97**(7), 073004 (2018). arXiv:1801.02007 [hep-ph]
24. R.N. Faustov, V.O. Galkin, Phys. Rev. D **98**(9), 093006 (2018). arXiv:1810.03388 [hep-ph]
25. T. Bhattacharya, V. Cirigliano, S.D. Cohen, A. Filipuzzi, M. Gonzalez-Alonso, M.L. Graesser, R. Gupta, H.W. Lin, Phys. Rev. D **85**, 054512 (2012). arXiv:1110.6448 [hep-ph]
26. V. Cirigliano, J. Jenkins, M. Gonzalez-Alonso, Nucl. Phys. B **830**, 95 (2010). arXiv:0908.1754 [hep-ph]
27. T. Gutsche, M.A. Ivanov, J.G. Körner, V.E. Lyubovitskij, P. Santorelli, N. Habyl. Phys. Rev. D **91**(7), 074001 (2015) Erratum: [Phys. Rev. D **91** (2015) no.11, 119907] arXiv:1502.04864 [hep-ph]
28. S. Shivashankara, W. Wu, A. Datta, Phys. Rev. D **91**(11), 115003 (2015). arXiv:1502.07230 [hep-ph]
29. X.Q. Li, Y.D. Yang, X. Zhang, JHEP **1702**, 068 (2017). arXiv:1611.01635 [hep-ph]
30. A. Celis, M. Jung, X.Q. Li, A. Pich, Phys. Lett. B **771**, 168 (2017). arXiv:1612.07757 [hep-ph]
31. R. Alonso, B. Grinstein, J. Martin Camalich, Phys. Rev. Lett. **118**(8), 081802 (2017). arXiv:1611.06676 [hep-ph]
32. Y. Sakaki, M. Tanaka, A. Tayduganov, R. Watanabe, Phys. Rev. D **88**(9), 094012 (2013). arXiv:1309.0301 [hep-ph]
33. M. Tanaka, R. Watanabe, Phys. Rev. D **87**(3), 034028 (2013). arXiv:1212.1878 [hep-ph]
34. J. A. Bailey et al. [Fermilab Lattice and MILC Collaborations], Phys. Rev. D **92**(1), 014024 (2015) arXiv:1503.07839 [hep-lat]
35. M.A. Ivanov, J.G. Körner, C.T. Tran, Phys. Rev. D **94**(9), 094028 (2016) arXiv:1607.02932 [hep-ph]
36. C.T. Tran, M.A. Ivanov, J.G. Körner, P. Santorelli, Phys. Rev. D **97**(5), 054014 (2018). arXiv:1801.06927 [hep-ph]
37. C. Murgui, A. Peñuelas, M. Jung, A. Pich, arXiv:1904.09311 [hep-ph]
38. M. Tanabashi et al. [Particle Data Group], Phys. Rev. D **98**(3), 030001 (2018)